remote sensing

MDPI

Article

A Cost-Effective GNSS Solution for Continuous Monitoring of Landslides

Veton Hamza *, Bojan Stopar, Oskar Sterle and Polona Pavlovčič-Prešeren

Faculty of Civil and Geodetic Engineering, University of Ljubljana, Jamova Cesta 2, 1000 Ljubljana, Slovenia; bojan.stopar@fgg.uni-lj.si (B.S.); oskar.sterle@fgg.uni-lj.si (O.S.); polona.pavlovcic-preseren@fgg.uni-lj.si (P.P.-P.)
* Correspondence: veton.hamza@fgg.uni-lj.si

Abstract: The development of low-cost dual-frequency global navigation satellite system (GNSS) receivers in recent years has enabled the use of these devices in numerous applications. In the monitoring of natural hazards, such as landslides, these devices can be considered suitable sensors. In this work, dual-frequency GNSS receivers and antennas were used for setting up near-real-time continuous low-cost GNSS monitoring systems (LGMSs) under field conditions. The SimpleRTK2B board, which integrates the u-blox ZED-F9P dual-frequency GNSS chip and the survey-calibrated GNSS antenna are the main components of the GNSS system. The LGMS was installed and tested for six months in the Laze landslide located in the northwestern part of Slovenia. A total of four GNSS systems were deployed, three of which were located in pillars in the landslide itself and one in a stable area. Open-source software was used to postprocess the acquired data, providing daily coordinates in static relative and precise point positioning (PPP) positioning modes. The results of six months of near-real-time monitoring showed that the Laze landslide was stable during this period, with only minor changes in the vertical component. The trend of decreasing ellipsoid height was evident at all stations, although it was in the range of a few millimeters. To validate the results in static relative positioning mode, the coordinate differences between low-cost and high-end geodetic GNSS instruments were estimated and found to be in the range of 5 mm or less, while the difference between horizontal and spatial positions was less than 7 mm for all stations. The same data were processed in PPP, vertical displacements were not detected as in the static relative positioning mode due to the lower accuracy of the method itself. Considering the six-month performance of a low-cost GNSS system under field conditions, it can be emphasized that these devices are capable of performing near real-time continuous monitoring of slow movements with high accuracy and decreased costs. In addition, an experimental test was performed to identify the size of detected displacements in real-time kinematic (RTK). Based on the achieved results, it was concluded that 20 mm spatial displacements are detectable with LGMSs in RTK considering only 15 s of observations.

Keywords: GNSS; monitoring; low-cost receivers; low-cost antennas; landslides

Citation: Hamza, V.; Stopar, B.; Sterle, O.; Pavlovčič-Prešeren, P. A Cost-Effective GNSS Solution for Continuous Monitoring of Landslides. *Remote Sens.* **2023**, *15*, 2287. https://doi.org/10.3390/rs15092287

Academic Editor: José Fernández

Received: 24 March 2023
Revised: 18 April 2023
Accepted: 24 April 2023
Published: 26 April 2023

1. Introduction

Global navigation satellite system (GNSS) receivers are widely used for geodetic monitoring applications, for which they are regarded as suitable sensors [1–4]. Geodetic GNSS devices have advantages over classical geodetic sensors when used in geodetic monitoring, as they can provide high-quality positioning solutions continuously in all weather conditions and with less effort. However, the use of geodetic GNSS devices in monitoring natural hazards such as landslides is not an optimal solution since those devices come with high costs; additionally, the possibility of instrument damage in such unstable areas is high [5–7].

Recently, low-cost dual-frequency GNSS receivers and calibrated multiband GNSS antennas have become available on the market [8,9]. Considering their price, these new sensors have triggered the interest of many researchers in the GNSS community and

are considered to be an alternative to high-quality geodetic GNSS instruments for many applications that have a limited budget.

1.1. Dual-Frequency Low-Cost GNSS Receivers

The positioning performance and data quality from low-cost dual-frequency GNSS receivers and antennas have been evaluated in numerous tests in recent years [10–15]. Most of these tests were carried out in open-sky conditions due to the sensitivity of the patch antennas used for multipath effects [5,16]. Later, these GNSS devices were evaluated in limited studies in urban areas and harsh conditions [17–20].

Within the study in [21], zenith tropospheric delay (ZTD) was estimated using the low-cost GNSS receiver ZED-F9P in combination with patch and geodetic antennas. It was found that these devices, after relative calibration of the u-blox patch antenna used, can obtain results for ZTD with quality comparable to that of geodetic GNSS antennas. The estimation of phase center offset (PCO) and phase center variations (PCVs) for low-cost antennas (u-blox ANN-MB-00) was shown to improve the carrier phase residuals and height errors while also obtaining more precise positioning solutions in precise point positioning (PPP) [22]. In the case of [18], low-cost dual-frequency receivers were tested in urban conditions, with static relative, PPP, and real-time Kinematic (RTK) positioning modes being considered. Positioning accuracies of a few centimeters were obtained in the static relative and PPP methods, while in the RTK, the positioning quality was worse compared to the value reported by the manufacturer. Romero-Andrade et al. [19] highlighted that dual-frequency receivers are suitable for surveying in urban areas, although the height component remains a challenge for patch antennas, which are more sensitive to multipath.

Low-cost dual-frequency GNSS receivers with calibrated low-cost antennas were evaluated for displacement detections in open-sky conditions, with both static relative and PPP methods being considered. Based on the obtained results, it was found that horizontal and spatial displacements of 4 and 6 mm can be detected in static relative positioning even through using low-cost GNSS antennas. The magnitude of the detected spatial displacements increased to 20 mm in PPP [7]. In the case of [5], u-blox patch antennas were considered while a geodetic GNSS instrument was used as a reference station. The size of detectable displacements in static relative positioning mode was 10 m, which is still satisfactory for many engineering applications.

In a few studies, low-cost GNSS receivers have been used for monitoring natural hazards [23,24], engineering structures [25–29], and even crustal deformation studies [30]. Notti et al. [24] conducted continuous monitoring of the slope which causes deformations in the Madonna del Sasso Sanctuary in Italy using low-cost GNSS devices. The results indicated that the sensors used can track slow movements and be used to better explain the behavior of various unstable objects.

Low-cost single-frequency GNSS receivers have been adopted in geodetic monitoring of landslides [31,32], and the data combination from GNSS and remote sensing technology has been shown to ensure more information for landslide dynamics [33,34]. In the case of [23], low-cost GNSS receivers were used to monitor a landslide over nine months, and monitoring was also performed in nearby points with a terrestrial positioning system to evaluate obtained results. It was concluded that the GNSS devices used were suitable for monitoring surface displacements of natural hazards and obtaining more details for the landslide surface dynamics. Lin et al. [6] evaluated the multisystem PPP for landslide monitoring and reported that the combined multisystem PPP fulfilled the centimetric positioning accuracy and therefore is applicable in landslide monitoring. Cina and Piras [35] showed that low-cost GNSS receivers can be adopted in landslide monitoring while their accuracy can be improved in the case of considering the external antenna, proper acquisition time of observations, and short baselines.

Manzini et al. [25] utilized low-cost single constellation GNSS receivers for structural health monitoring of Aquitaine Bridge, France. First, several tests were performed to evaluate different antennas and processing strategies. The results of the experimental work

showed that subcentimetric displacements can be detected over short baselines and good weather conditions. Subsequently, some low-cost GNSS stations were installed on the bridge to monitor the movements for two weeks. The results were worse than those of the experimental work due to the weather conditions, the humidity caused by the water down on the bridge, and the complexity of the structure itself. Poluzzi et al. [29] assembled a low-cost monitoring system using low-cost GNSS devices (C94-M8P) and a Trimble Bullet 360° antenna to perform monitoring of the Ponte Motta Bridge in Cavezzo, Italy. The low-cost monitoring system was evaluated in both static relative and RTK methods for 31 days with two different open-source software packages being used for data processing. The uncertainties of the daily coordinates were 1 and 1–1.5 mm for a horizontal and vertical component in the static relative method, respectively. Higher uncertainties were obtained in RTK, remaining below 10 mm for both components. In the case of [28], low-cost GNSS instruments (LEA-6T receiver, Tallysman TW3742, and Tallysman 3740 antennas) were used to estimate the movements of an ancient structure (San Gaudenzio's Cupola, Italy) for more than one year. Movements of 2 cm in the vertical direction (during summer) were detected, followed by horizontal movements of less than 0.5 cm due to temperature variations.

In another study [30], a low-cost GNSS receiver (ZED-F9P) combined with a geodetic antenna (Leica LEIAR20) was evaluated for its suitability in crustal deformation studies. Two other GNSS receivers (Topcon TPS NETG5 and Leica GR25) were used as references to compare the results. Data were collected for six months, and daily coordinates were obtained using open-source software in ITRF08. The results indicated that low-cost GNSS receivers can provide coordinates with a precision of less than 1 mm for the horizontal component and 2.5 mm for the vertical component. The differences between the coordinates obtained by ZED-F9P and high-quality receivers were in the range of 1–2 mm and 5–8 mm for the horizontal and vertical components, respectively. Therefore, the authors emphasized that these devices can also be used for crustal deformation studies. Lastly, Hohensinn et al. [36] tested the performance of ZED-F9P with a patch antenna (u-blox ANN-MB), a helical antenna (Ardusimple), and a geodetic antenna (JAVAD GrAntT-G3T) in real-time PPP for kinematic monitoring applications. It was highlighted that ZED-F9P with helical antenna can obtain positioning with a quality comparable to that of high-grade GNSS devices. The authors suggested that these devices can be used to detect ground motion in the centimeter range and therefore can be used in the field of seismology and earthquake warning.

1.2. Objective and Study Organization

In this study, a low-cost dual-frequency GNSS receiver ZED-F9P that was integrated into simpleRTK2B board in combination with a survey-calibrated GNSS antenna was tested for continuous near-real-time geodetic monitoring of an active landslide (Laze) in Slovenia. The main objectives of the study were twofold: to test the capability of low-cost GNSS equipment for setting up a low-cost GNSS monitoring system (LGMS) under real field conditions and to analyze the size of detectable displacements in RTK.

This paper is organized as follows: Section 1 presents an overview of the use of low-cost dual-frequency GNSS receivers in various applications; Section 2 presents the case study, GNSS equipment, and methods used; Section 3 presents the results and discussion; and Section 4 lists the derived conclusions.

2. Material and Methods

2.1. Laze Landslide

The Laze landslide is located in the northwestern part of Slovenia, 35 km northwest of Ljubljana, more precisely between Robidnica (west) and Leskovica (east) (Figure 1). It occupies an area of 105.5 ha and has the shape of the letter S with a slope of 10° (Figure 1). The landslide is divided into two parts: the upper part, which is more active; and the lower part in the village of Laze, which poses a direct threat to buildings, local roads, and residents. Precipitation is the main triggering factor for landsliding in Slovenia. Ac-

cording to the observations from Slovenian Environment Agency (ARSO), the average precipitation in the Leskovica station, which is the nearest one to the Laze landslide, is about 1700 mm/year [37]. Usually, the movements occur after heavy rainfall. The largest movement took place in January 2014, and after that, various activities and investigations started [38].

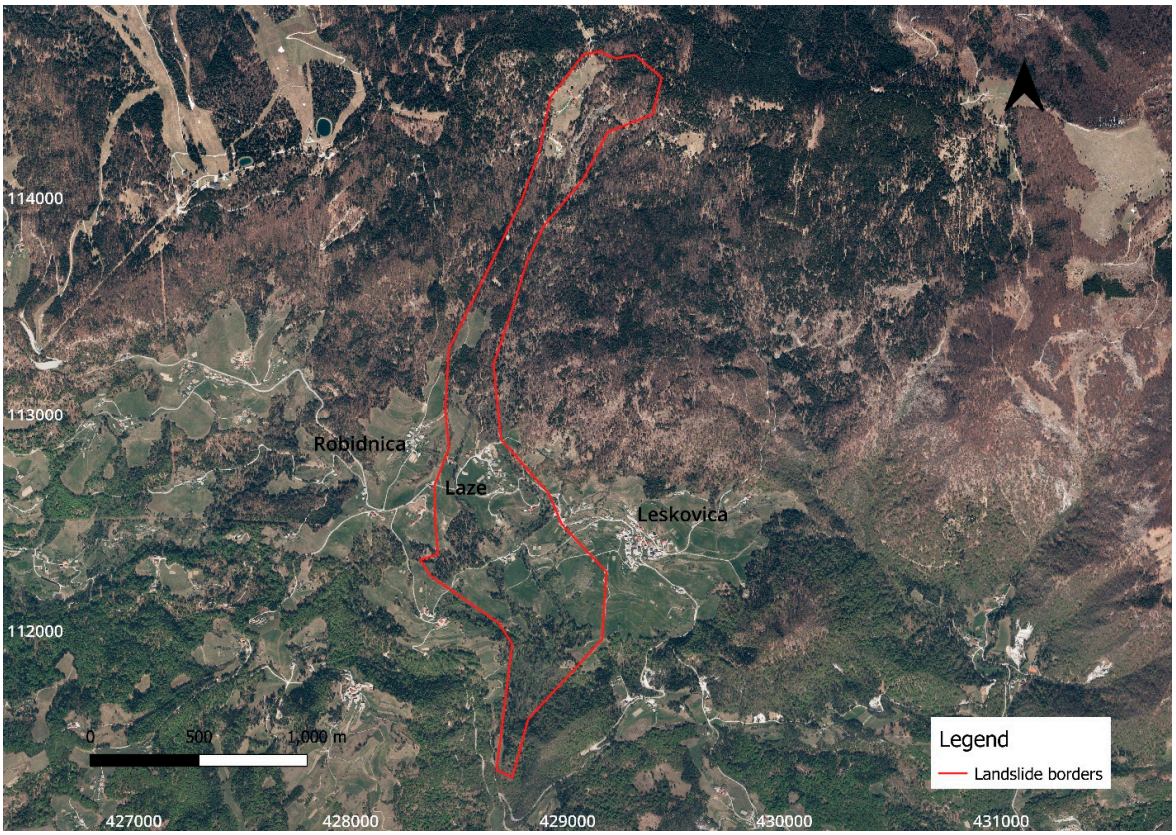

Figure 1. Laze landslide location and shape.

Initially, monitoring was conducted only by visual inspections, then some boreholes were drilled in 2014 to determine the landslide depths, and later larger boreholes were installed in 2015 with equipment to pump out the water and measure the groundwater level. Lastly, three monitoring stations (Figure 2) that can perform tilt measurements were mounted, which can also send an alarm when deep displacements occur [38].

Figure 2. Measuring station used for tilt measurements.

2.2. Geodetic Network

In 2016, the geodetic monitoring network was established, and it consists of seven pillars with force-centering systems. Five pillars are located in the stable area near the village of Laze (STI to STV) and can be used for GNSS observations. Due to vegetation and trees, only two of them (STI and STII) have a good sky view for continuous GNSS observations throughout the year (Figure 3). Later, in spring 2021, two additional pillars were constructed in the lower part of the landslide. In addition, there are more than 80 ground geodetic points that are measured periodically with GNSS devices to estimate displacements. The geodetic network used in this work consists of four points and six baseline vectors (Figure 3). STI has been used as a known point, while the coordinates of stations ST1, ST2, and ST3 are estimated for each day.

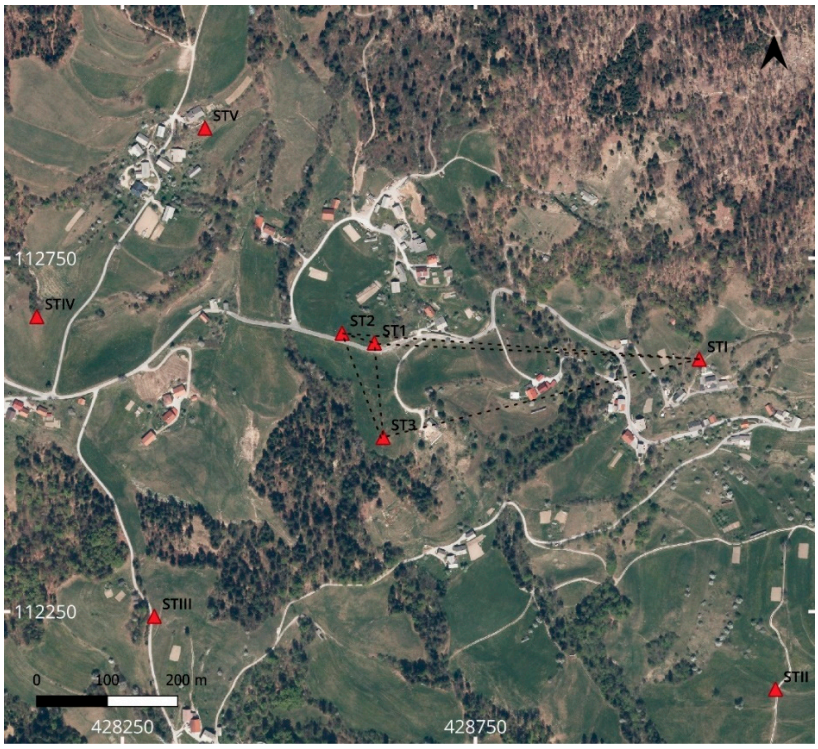

Figure 3. Geodetic network in the Laze landslide.

2.3. GNSS Equipment

The market for low-cost GNSS receivers has grown rapidly in recent years, and several manufacturers now offer low-cost GNSS devices at low prices. The u-blox company, which has been in the market for many years, has developed the ninth generation of low-cost receivers, with the ZED-F9P classified as a high-precision GNSS module [9]. This was an interesting moment for the GNSS community, as high-quality positioning, could be achieved at a low cost (170 EUR). The ZED-F9P GNSS chip is integrated into various GNSS boards such as the C099-F9P (u-blox), simpleRTK2B (Ardusimple), SparkFun GPS-RTK2 (Sparkfun), and others.

In this case study, we used simpleRTK2B (Figure 4a) as the main component to build up the LGMS. The ZED-F9P can receive satellite signals in both frequencies from all constellations and output UBX messages which can be converted to RINEX format for further processing. The board was connected by cable to the dual-band survey-calibrated GNSS antenna (Figure 4b). A solar panel (25 W) was used to charge a lithium battery with a capacity of 30 Ah. The power consumption of the low-cost GNSS equipment used is low, and the battery used can provide power for more than a week when fully charged. The cost of an LGMS did not exceed the value of 500 EUR. The installed LGMSs are shown for all stations in Figure 5 while more details for used equipment are given in Table 1.

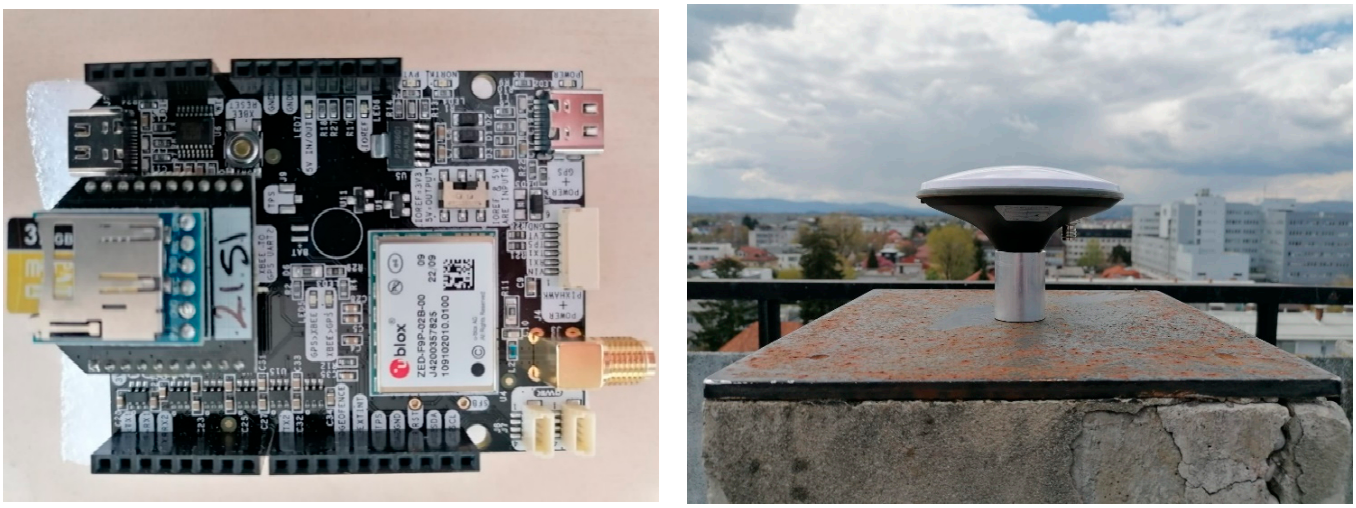

(**a**) (**b**)

Figure 4. GNSS equipment: (**a**) SimpleRTK2B receiver and (**b**) the survey-calibrated GNSS antenna.

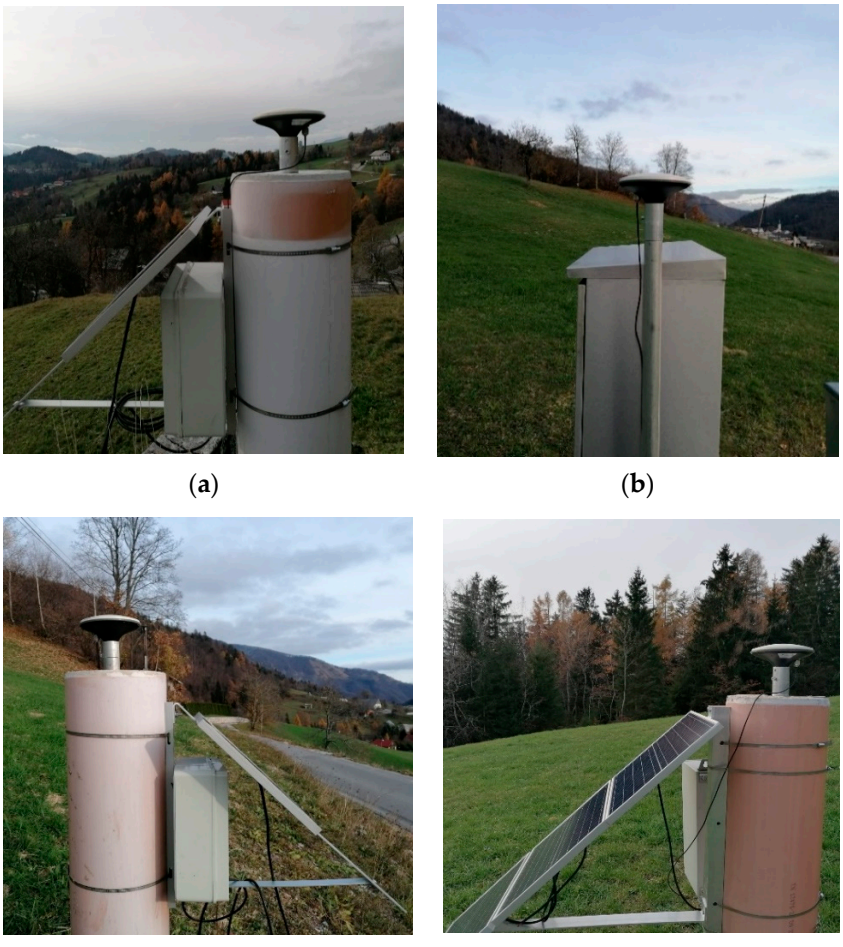

(**a**) (**b**)

(**c**) (**d**)

Figure 5. LGMS installed in the Laze landslide: (**a**) LGMS in ST I, (**b**) LGMS in ST 1, (**c**) LGMS in ST 2, and (**d**) LGMS in ST 3.

Table 1. Specifications for LGMS.

Characteristics	
GNSS board	SimpleRTK2B
GNSS antenna	Survey Calibrated GNSS antenna
Constellations and frequencies	GPS (L1C/A, L2C), GLONASS (L1OF, L2OF), Galileo (E1-b/C, E5b), BeiDou (B1l, B2l), QZSS (L1C/A, L2C)
Observations	Code, Carrier phase, Doppler frequency, SNR
Channels	184
Antenna calibration	Yes (NGS)
Configuration	U-center
Data storage	32GB
Basic system price	500 EUR
Operating temperature	−40 to +85 °C
Interfaces	Micro USB, UART
Raw messages	UBX
Positioning accuracy	Hz, Hv < 1 cm, 1 km baseline, RTKLIB postprocessing
Power consumption	150 mA@5 V
Antenna IP rating	IP67
Solar panel	25 W
Lithium battery	30 Ah, 12 V

2.4. Data Processing

To estimate the movements of points on the landslide and test the functionality of LGMS under field conditions, GNSS static observations were acquired for six months starting on 25 March 2022. The UBX messages outputted by the receiver were converted to RINEX format. The point ST I was used as a reference point, the initial coordinates of which were estimated in the static relative processing method from the observations acquired with Slovenian Continuously Operation Reference Stations (CORS) and high-quality geodetic GNSS receivers (Leica GS18T). The coordinates of the other points (ST1, ST2, and ST3) were estimated for each day based on 24 h observations to achieve the highest possible precision, and the minimally constrained geodetic network adjustment was performed while the following conditions were fulfilled:

$$v_i^T P_i v_i = min, \quad (1)$$

where v_i and P_i are the residual vector and weight matrix for the i-th session, respectively. For outlier detection, the data screening method was used with a significance level of 5%. Baseline vector postprocessing was conducted by using the open-source software RTKLIB by using the parameters provided in Table 2 [39].

Table 2. Parameters used for baseline processing in RTKLIB [39].

Parameters	RTKLIB
Filter type	Combined
Elevation mask	10°
Iono correction	Broadcast
Troposphere correction	Sastamoinen
Satellite ephemeris/clock	Broadcast
Ambiguity	Continuous
Satellites	GPS, GLO, Galileo
Antenna	AS-ANT2BCAL

Daily coordinates for points in the landslide body were also estimated in PPP. MGEX products, precise ephemerides (15 min), and clock corrections (30 s) were considered; the "igs.atx" (IGS) file was used for receiver and satellite phase center variations [40]. The tropospheric delay was corrected with the "Estimated ZTD" model, while for the ionospheric error the "Iono-Free", model LC was considered.

To validate the LGMS static relative positioning performance, the same geodetic network was measured with high-ended geodetic GNSS receivers (Leica GS18T) for 5 h at 1 Hz on 23 June 2022, and afterward, the minimally constrained adjustment was performed. The difference in the coordinates obtained from geodetic (e_G-easting, n_G-northing, h_G-ellipsoid height) and low-cost GNSS receivers (e_{LC}-easting, n_{LC}-northing, h_{LC}-ellipsoid height), and the horizontal and spatial positions were estimated as follows:

$$\Delta h = h_{LC} - h_G \tag{2}$$

$$\Delta e = e_{LC} - e_G \tag{3}$$

$$\Delta n = n_{LC} - n_G \tag{4}$$

$$\Delta_{2D} = \sqrt{\Delta e^2 + \Delta n^2} \tag{5}$$

$$\Delta_{3D} = \sqrt{\Delta e^2 + \Delta n^2 + \Delta h^2} \tag{6}$$

2.5. Rainfall Data

Precipitation is the main triggering factor for the movements in the Laze landslide [38]. Therefore, daily precipitation data from the Leskovica station were used to analyze whether certain movements occur after rainy days. Dry conditions lasted from spring through summer, and states of drought emergency were declared in all parts of the country. The drought was over after heavy rains in mid-September that lasted for three days.

2.6. RTK Displacement Detection

The RTK engine of LGMS was additionally tested for displacement detection while a mechanical device was used to impose controlled movements with high accuracy on the rooftop of the Faculty of Civil and Geodetic Engineering of the University of Ljubljana building (Figure 6). The imposed movements were in the range of 5–55 mm, while the test aimed to identify the smallest displacements that can be detected in RTK. In total, 22 positions were observed, and each position was measured for 15 s only. The distance between consecutive positions was 5 mm while the time difference was 20 min to account for changes in satellite geometry. The CORS base station named GSR1, located 4 km far from the rover named FGG1, was used to provide corrections. Additionally, we used the virtual reference station (VRS) generated from the CORS of the SIGNAL network, which used GNSS observation from the GPS, GLONASS, and Galileo satellite constellations. The VRS was generated approximately 2 m from the rover FGG1 to analyze the improvement in the size of the detectable displacements.

To determine the statistical significance of the estimated 1D vertical, 2D horizontal, and 3D spatial movements, statistical tests were used [41–43], and the following hypotheses were set:

H_0. *$d = 0$, Point remained stable between sessions.*

H_A. *$d \neq 0$; Point moved between sessions.*

The rejection of the null hypothesis was analyzed with the following statistical test [41]:

$$T = \frac{d}{\sigma_d} \tag{7}$$

Imposed movements (d) were calculated from the provided coordinates of each measured position as follows:

$$d_{1D} = h_i - h_j \tag{8}$$

$$d_{2D} = \sqrt{\left(e_i - e_j\right)^2 + \left(n_i - n_j\right)^2} \tag{9}$$

$$d_{3D} = \sqrt{\left(e_i - e_j\right)^2 + \left(n_i - n_j\right)^2 + \left(h_i - h_j\right)^2} \tag{10}$$

where the e_i, n_i, h_i and e_j, n_j, h_j are the coordinates of positions used to calculate the displacement. The displacement precision (σ_d) and 1D, 2D, and 3D Jacobi matrices were estimated based on the error propagation law; more details are provided in [44]. The estimated value of the statistical test (T) was compared with its corresponding critical value from the normal (N, in the case of 1D displacements) and chi-squared (χ^2, in the case of 2D and 3D displacements) distributions. The critical values were defined based on the displacement dimension: the critical values were 1.96, 2.45, and 2.80 for the 1D, 2D, and 3D displacements, respectively, for a significance level of 5% (α = 0.05).

Figure 6. Special device for imposing controlled movements.

Considering that movements were imposed with high accuracy (0.05 mm), their true values are well known. The mean absolute error (MAE) was estimated for all imposed 1D, 2D, and 3D movements for both baselines.

3. Results and Discussion

In this section, the results of the previous section are shown: first, for static relative method (Section 3.1); then forPPP method (Section 3.2) and rainfall (Section 3.3); and finally for RTK displacement detection (Section 3.4).

3.1. Static Relative Method

The LGMS was tested in the Laze landslide for six months starting on 25 March 2022, and the equipment used worked properly and continuously. However, some difficulties

were encountered at ST2, where no observations could be recorded for three weeks due to technical problems with SimpleRTK2B, which were later resolved by installing a new GNSS receiver. Based on the tests performed, it can be stated that the power consumption of the LGMS is too low. The solar panels (25 W) used and the battery (30 Ah) were able to provide power during the whole period.

In the static relative processing method, daily coordinate differences (Figure 7) for easting (Δe), northing (Δn), and ellipsoid height (Δh) were estimated for ST1, ST2, and ST3 from the coordinates which were calculated with submillimeter precision. Variations of the horizontal coordinate differences (Δe and Δn) were in the range of ± 5 mm or even lower for all stations. Somewhat larger variations were determined for the ellipsoid height (Δh) (Figure 7), which decreased continuously and slowly at all three stations, although this was more evident at ST2, where the difference reached a value of almost 10 mm.

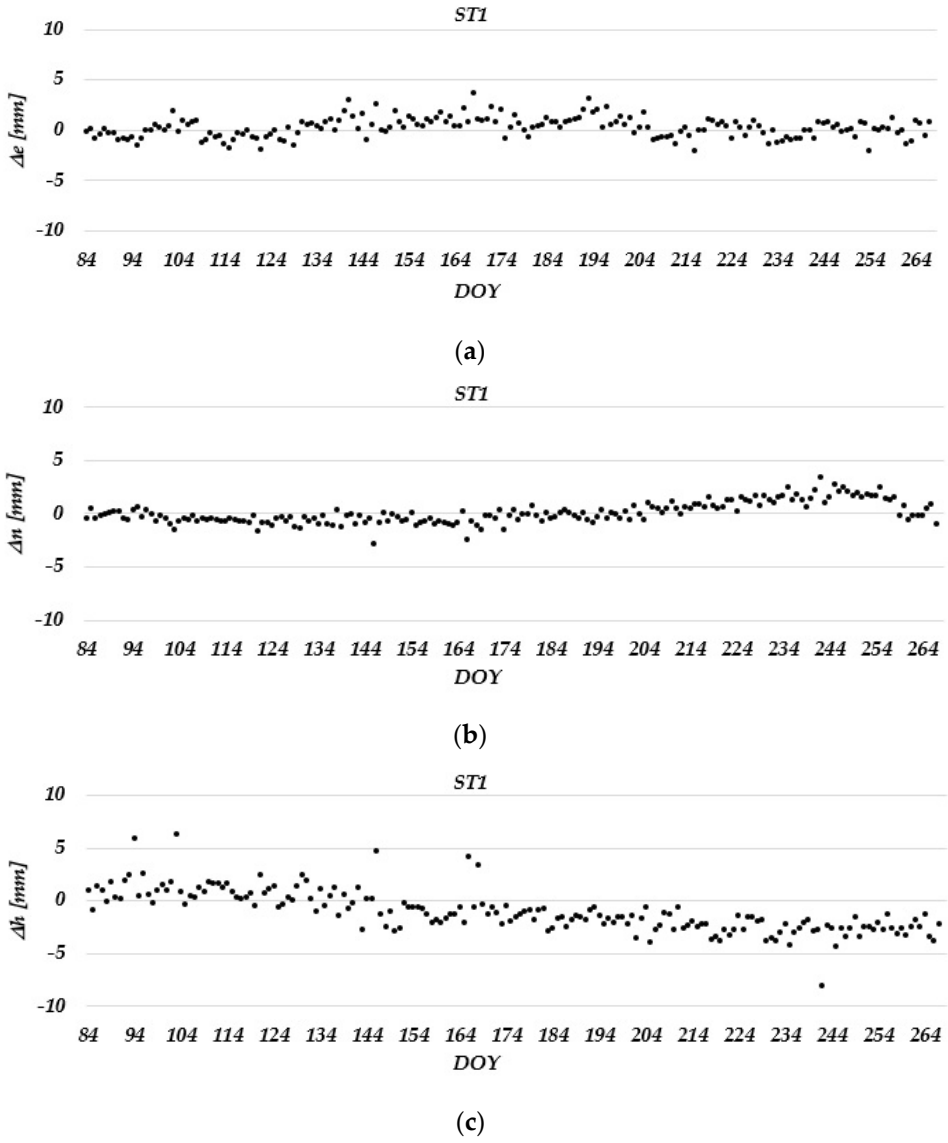

Figure 7. *Cont.*

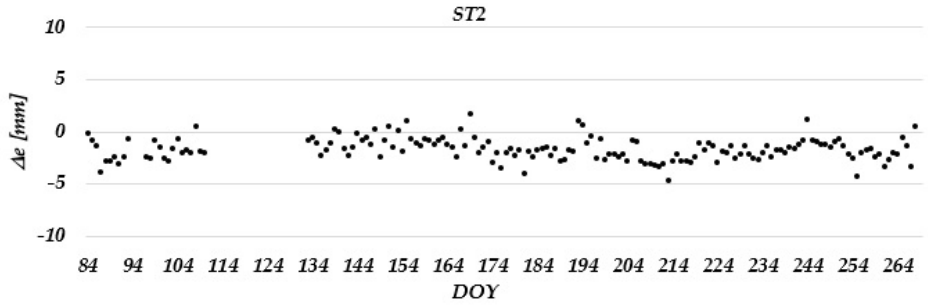

(**d**)

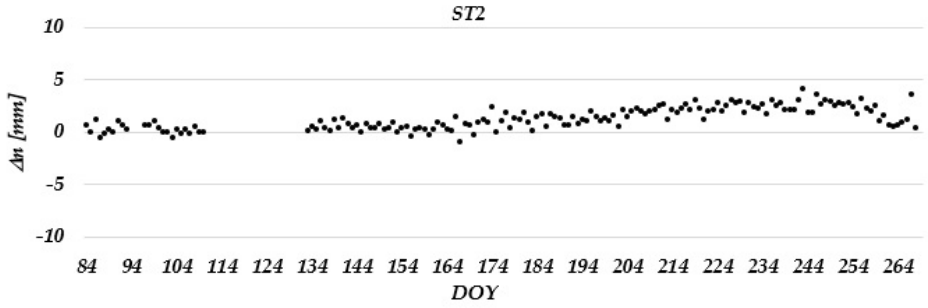

(**e**)

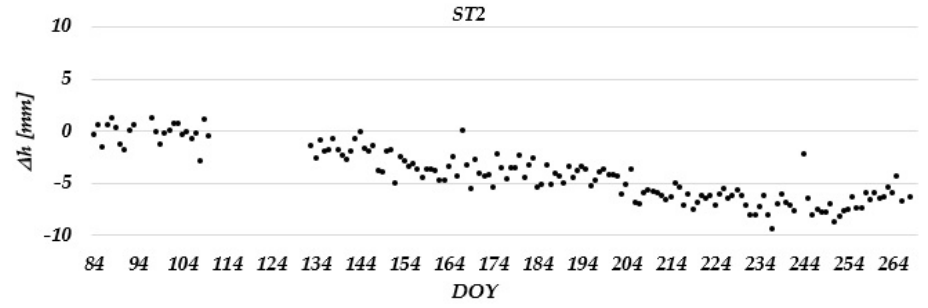

(**f**)

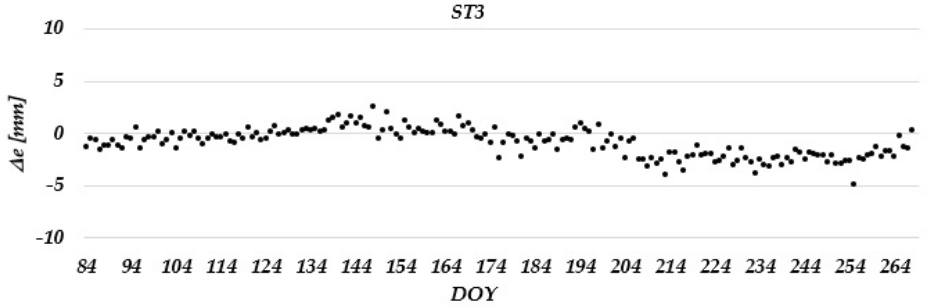

(**g**)

Figure 7. *Cont.*

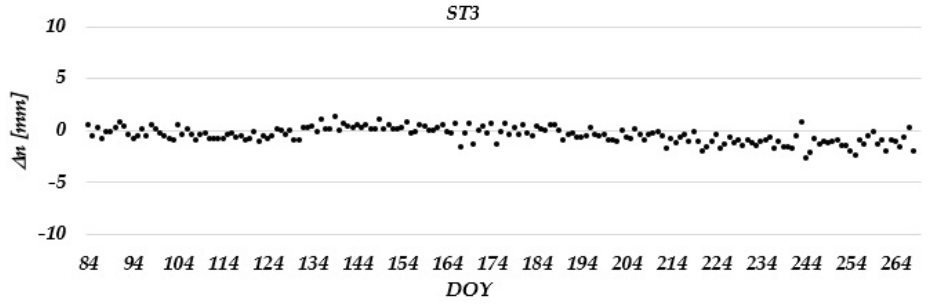

(**h**)

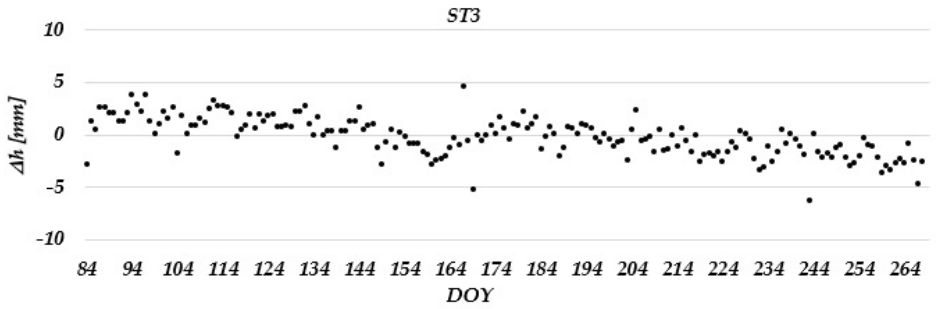

(**i**)

Figure 7. Coordinate differences for ST 1, ST2, and ST3 obtained in static relative method: (**a**) Δ*e* ST1, (**b**) Δ*n* ST1, (**c**) Δ*h* ST1, (**d**) Δ*e* ST2, (**e**) Δ*n* ST2, (**f**) Δ*h* ST2, (**g**) Δ*e* ST3, (**h**) Δ*n* ST3, and (**i**) Δ*h* ST3.

To compare the results provided by the LGMS in the static relative positioning mode, additional observations were conducted with GNSS geodetic instruments, and the coordinate differences were estimated (Table 3). The results show that the coordinate differences for easting, northing, and ellipsoid height were less than 6 mm and are within the accuracy range of GNSS technology (Table 3). The differences between geodetic and low-cost GNSS instruments for horizontal and spatial positions were in the range of 5–7 mm (Table 3).

Table 3. Coordinate differences between low-cost and geodetic GNSS devices.

Station	Δ*e*	Δ*n*	Δ*h*	Δ2D	Δ3D
Station 1	−2.7 mm	3.7 mm	0.2 mm	4.6 mm	4.6 mm
Station 2	−2.3 mm	6.0 mm	0.1 mm	6.3 mm	6.3 mm
Station 3	−4.8 mm	4.9 mm	−0.8 mm	6.9 mm	6.9 mm

Horizontal displacements (estimated from the initial and following positions) remained below 5 mm for all three stations and are presented in their absolute values, while the vertical displacements (Δ*h*) following a decreasing trend, which is further highlighted in ST2 (Figure 8).

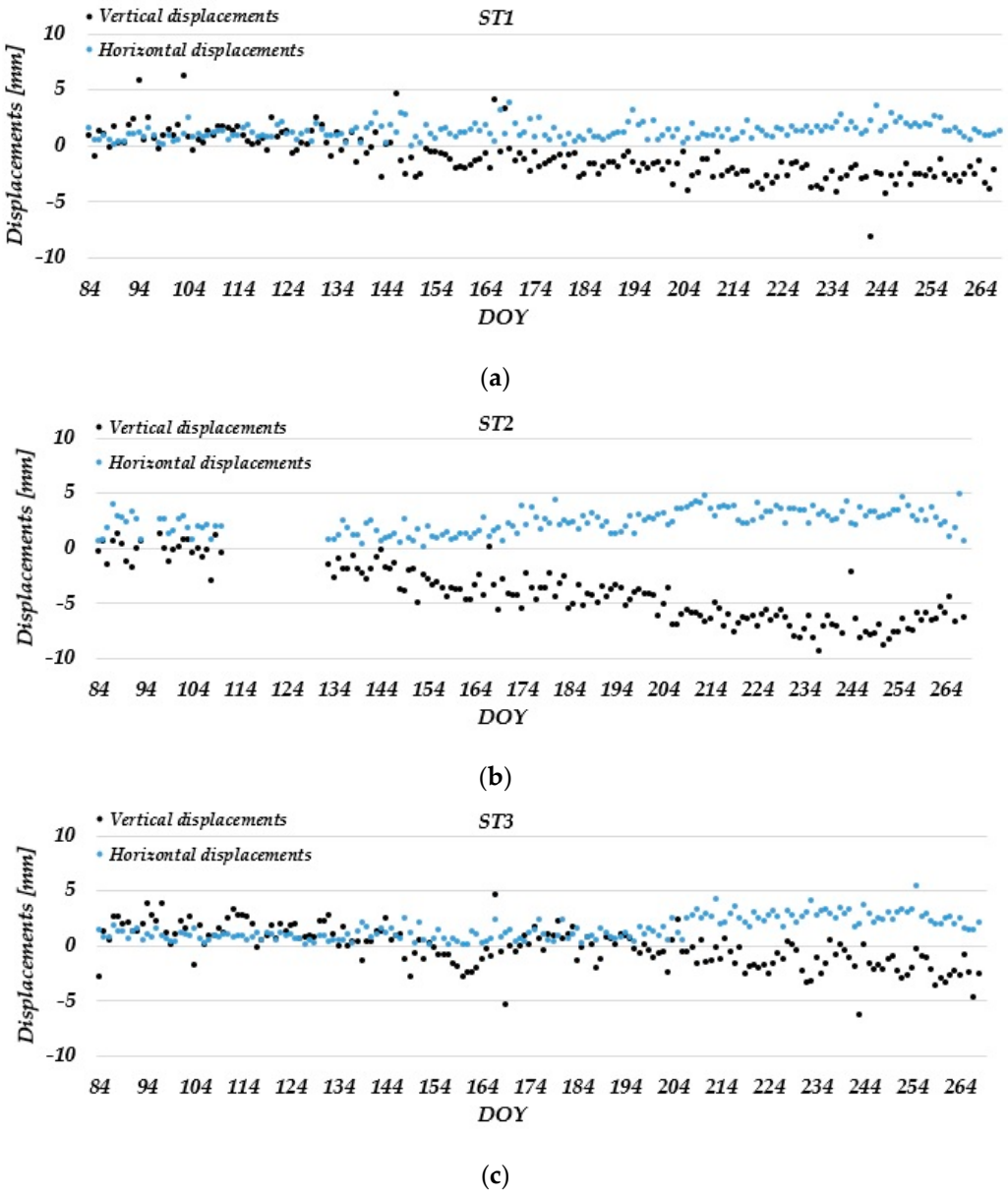

Figure 8. Horizontal and vertical displacements obtained in static relative method: (**a**) ST1, (**b**) ST2, and (**c**) ST3.

3.2. PPP Method

The acquired observations for six months were processed in PPP for ST1, ST2, and ST3 which are shown in Figure 9. Similar results as those derived from static relative processing were obtained for the horizontal and vertical displacements (Figure 10).

The precision of position determination in PPP was lower than that in static relative positioning mode. Variations of the daily coordinate differences are higher for all stations, especially for the easting value of ST2. Considering the lower quality of the PPP solutions, the decreasing trend for the ellipsoid height was not noticeable (Figure 9). Similar results were obtained for the horizontal and vertical displacements; again, the displacements were slightly larger in ST2, which was due to larger variations in the daily east coordinate differences for ST2 (Figure 10). This could be related to the technical problems we had with the GNSS receiver itself. However, after installing the new GNSS receiver, the coordinate differences decreased and were similar to the variations in ST1 and ST3 (Figure 9).

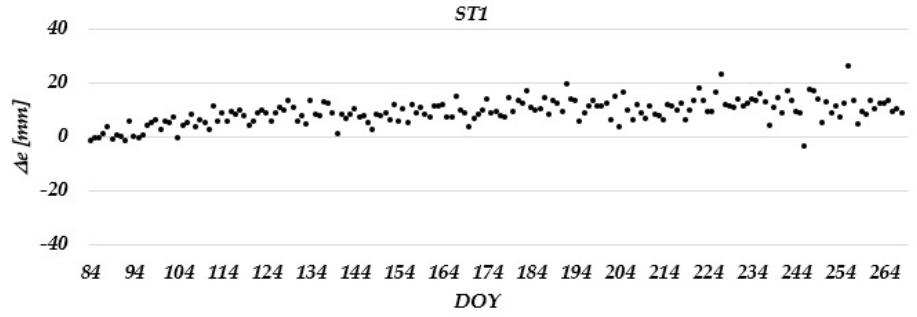

(**a**)

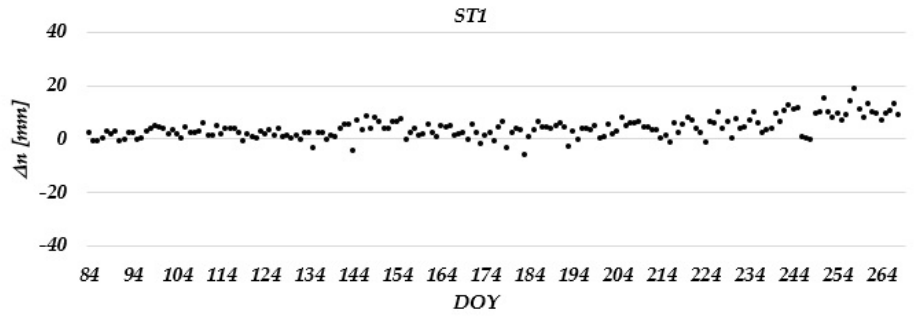

(**b**)

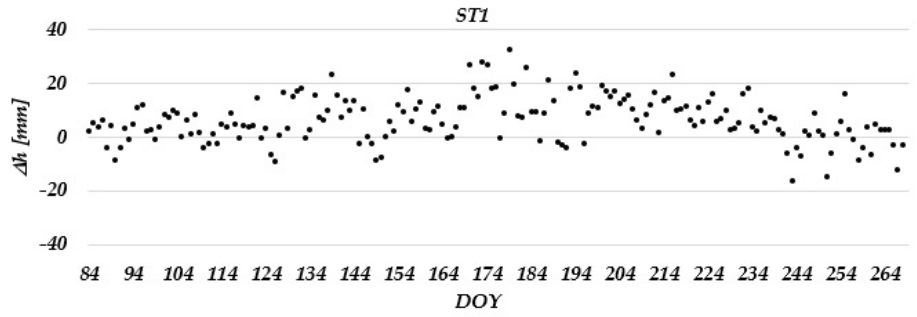

(**c**)

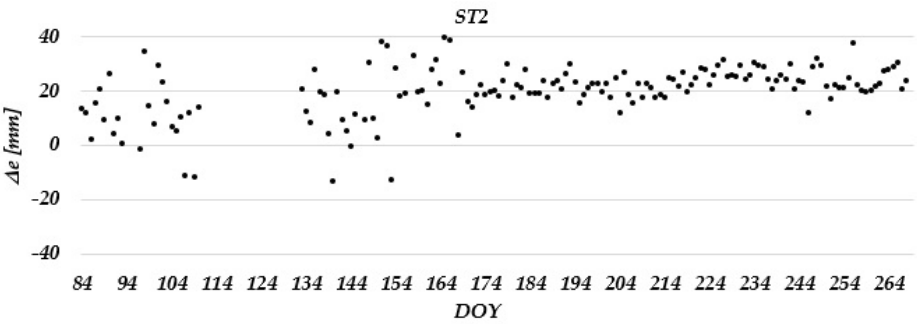

(**d**)

Figure 9. *Cont.*

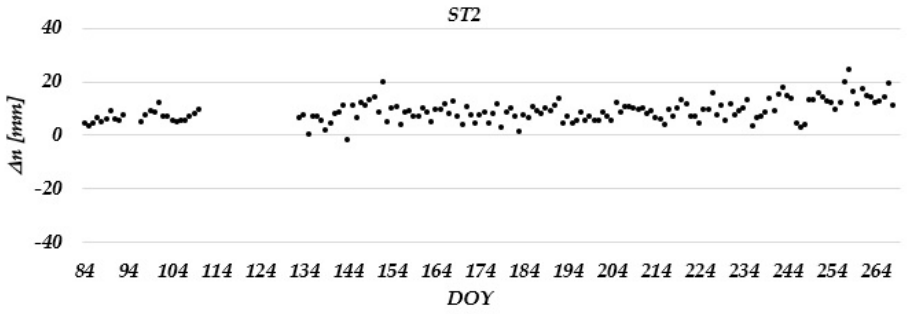

(**e**)

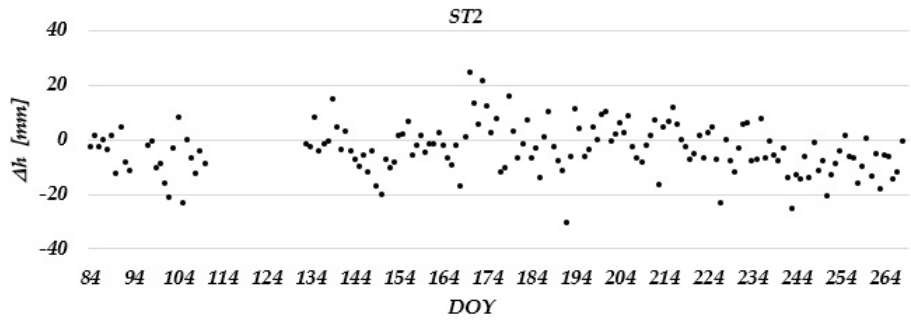

(**f**)

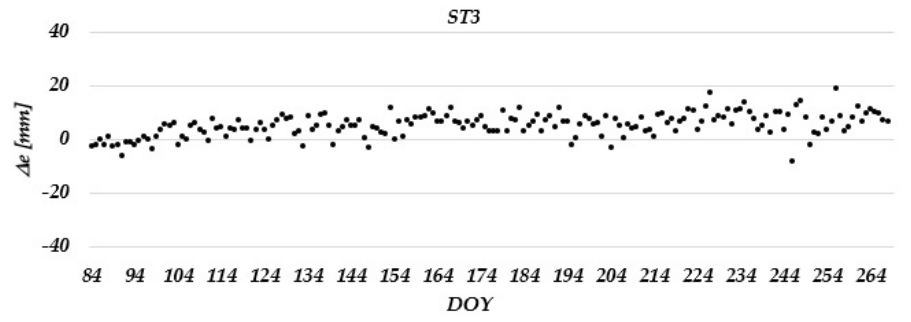

(**g**)

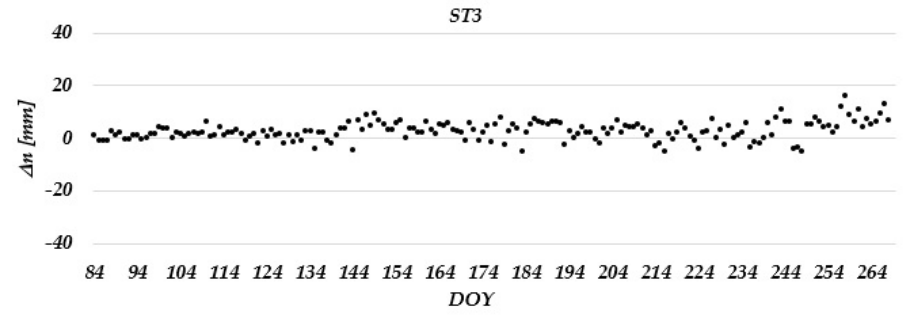

(**h**)

Figure 9. *Cont.*

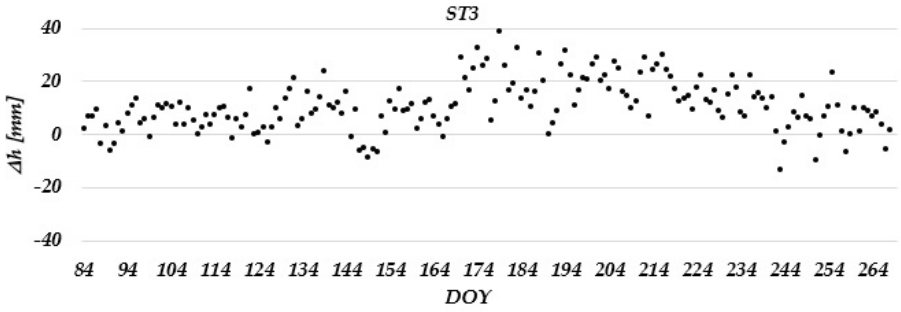

(**i**)

Figure 9. Coordinate differences for ST1, ST2, and ST3 in PPP: (**a**) Δ*e* ST1, (**b**) Δ*n* ST1, (**c**) Δ*h* ST1, (**d**) Δ*e* ST2, (**e**) Δ*n* ST2, (**f**) Δ*h* ST2, (**g**) Δ*e* ST3, (**h**) Δ*n* ST3, and (**i**) Δ*h* ST3.

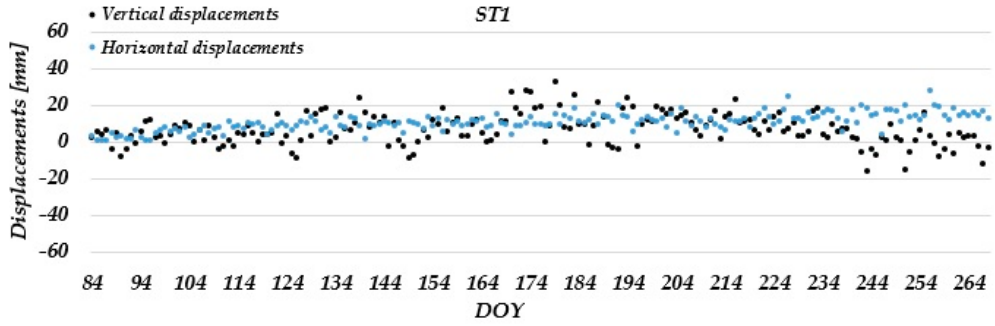

(**a**)

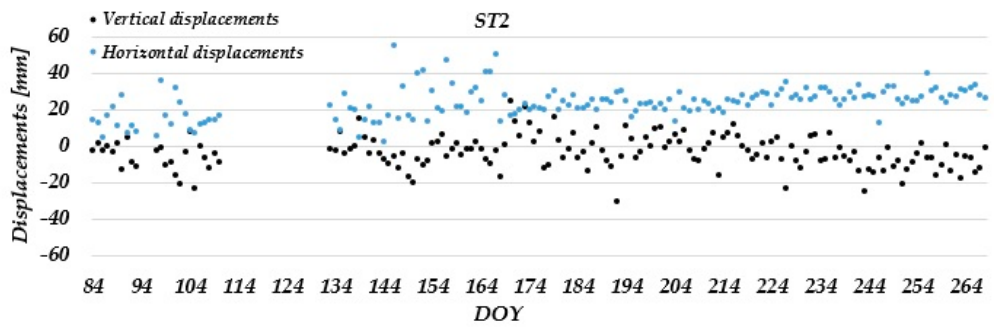

(**b**)

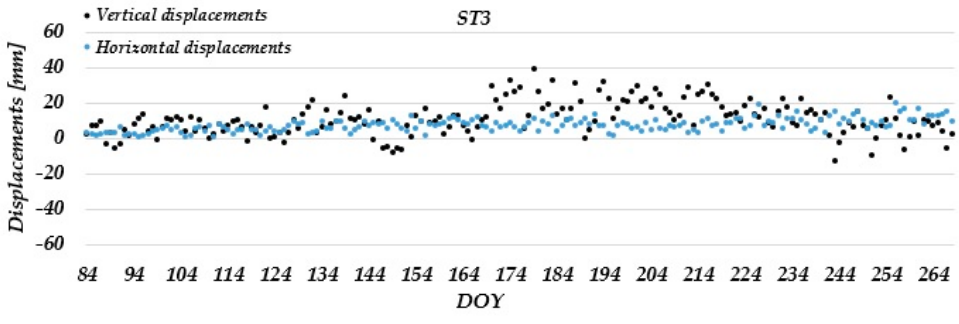

(**c**)

Figure 10. Horizontal and vertical displacements in PPP: (**a**) ST1, (**b**) ST2, and (**c**) ST3.

3.3. Rainfall

Precipitation data from the Leskovica station were used to relate the possible displacements to precipitation. The precipitation data showed that the rainfall in 2022 was below average in almost all months. The drought conditions continued throughout the summer when a state of emergency was declared due to the extreme drought, ending in mid-September with extreme rain. During the monitoring period, there were only three rainy days when precipitation exceeded 40 mm (Figure 11, red bars). From 16 September 2022 to 18 September 2022, 210 mm of rain was recorded on three days due to continuous rain, which is almost half of the value for the entire monitoring period (519 mm) [37].

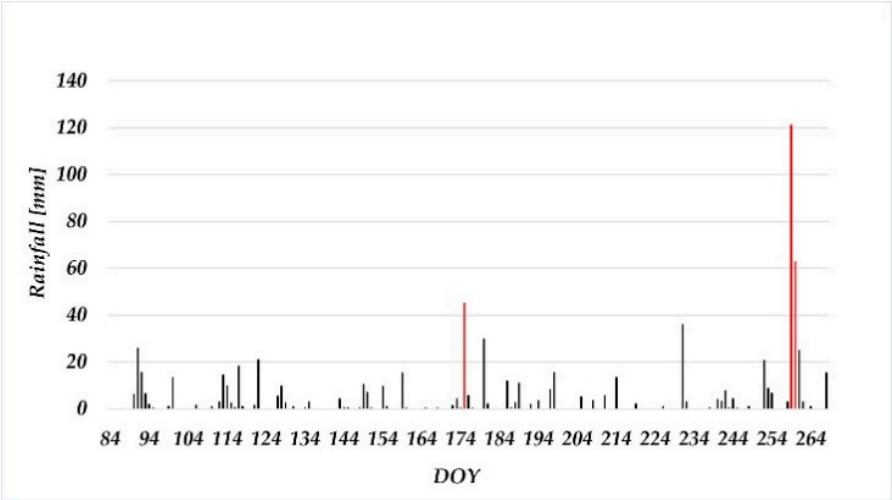

Figure 11. Precipitation at the Leskovica station.

Precipitation is a trigger factor for the movements in the Laze landslide [38]. The presented results emphasized that seven days after the record precipitation, no displacement occurred and the coordinate trend continued as previously.

3.4. RTK Displacement Detection

In this section, results from the statistical tests used in the 1D, 2D, and 3D displacement detection are presented in Tables 4–6, respectively. In the case of 1D displacements, the rover antenna was not moved vertically; therefore, we failed to reject the null hypothesis. As seen in the results presented in Table 5, there was no significant difference in displacement detection when using GSR1 or VRS as a reference station. However, the results confirmed that in more than 90% of the cases (276 imposed displacements), no displacement was detected.

Table 4. Vertical displacement (1D) detection results.

Station	GSR1-FGG1	VRS-FGG1
Not detected	95%	94%
Detected	5%	6%

Table 5. Horizontal displacements (2D) detection results.

Displacements	GSR1-FGG1	VRS-FGG1
5 mm	7%	0%
10 mm	28%	30%
15 mm	79%	81%
20 mm	94%	100%
25 mm	100%	100%

Table 6. Spatial displacements (3D) detection results.

Displacements	GSR1-FGG1	VRS-FGG1
5 mm	9%	2%
10 mm	25%	15%
15 mm	56%	75%
20 mm	97%	100%
25 mm	100%	100%

In the case of horizontal (2D) and spatial displacement (3D) detection, displacements of 20 mm or greater were successfully detected in more than 90% of the considered movements (248 imposed movements). On the other hand, displacements greater than 25 mm are not presented because all of them were reliably detected. A slightly better performance is noticed for the VRS-FGG1 baseline, but the difference was not significant (Tables 5 and 6).

The MAE of the imposed displacements represents their accuracy (Table 7), and displacements were estimated with subcentimetric precision in RTK. Based on the presented results (Table 7), it can be emphasized that better performance was achieved for baseline VRS-FGG1. The MAE of the 2D displacements was lower than that of the 3D displacements due to the error in the height component. In the case of 1D displacements, the values were higher than those of 2D and 3D since the number of imposed movements was not the same. The differences between the estimated 1D, 2D, and 3D displacements from their true values are presented graphically in Figure 12 from where it can be noticed that greater variations were obtained for the GSR1-FGG1 baseline which corroborates the results presented in Table 7.

Table 7. Mean absolute error (MAE) for the 1D, 2D, and 3D displacements.

Antenna	GSR1-FGG1			VRS-FGG1		
Dimension	1D	2D	3D	1D	2D	3D
MAE (mm)	7.7	4.0	4.3	5.8	2.4	3.5

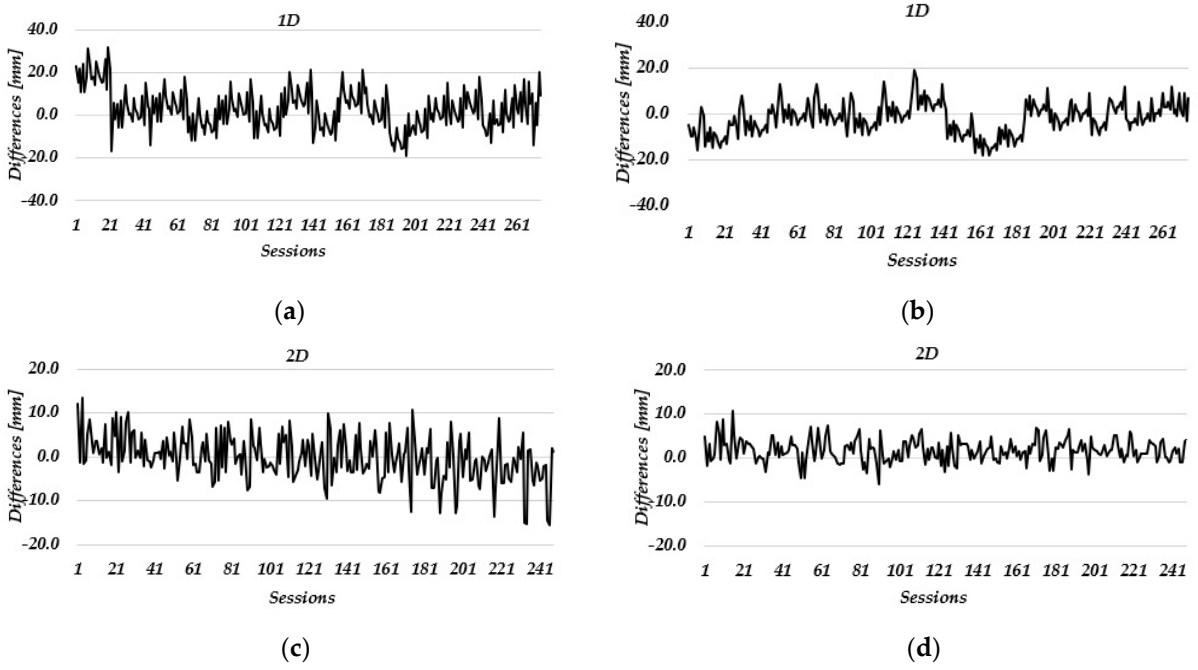

Figure 12. *Cont.*

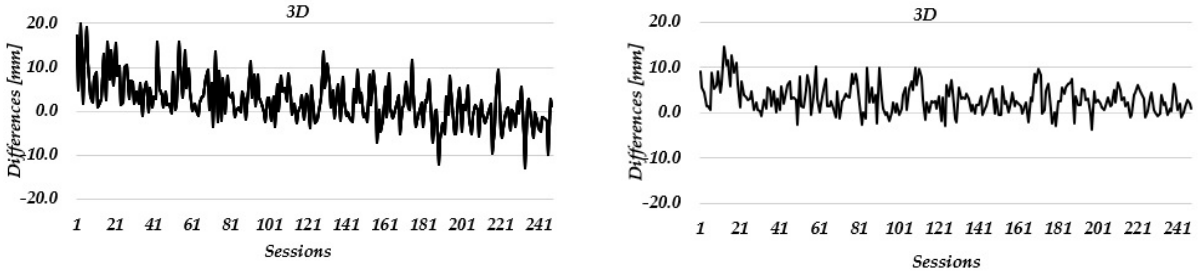

(**e**) (**f**)

Figure 12. 1D, 2D, and 3D differences between estimated and true displacements in RTK: (**a**) 1D, GSR1−FGG1 baseline; (**b**) 1D, VRS−FGG1 baseline; (**c**) 2D, GSR1−FGG1 baseline; (**d**) 2D, VRS−FGG1 baseline; (**e**) 3D, GSR1−FGG1 baseline; and (**f**) 3D, VRS−FGG1 baseline.

4. Conclusions

In this work, low-cost dual-frequency GNSS receivers and antennas were tested to set up a low-cost GNSS monitoring system for near-real-time continuous monitoring under field conditions. The Laze landslide, located in northwestern Slovenia, was selected as a case study for conducting the six-month test. The following conclusions can be drawn from the results obtained:

- Low-cost GNSS receivers are suitable for setting up a low-cost GNSS monitoring system with high positioning accuracy and provide near-real-time continuous monitoring of landslides or other buildings while meeting the accuracy requirements.
- Low-cost GNSS instruments are several times cheaper than are geodetic instruments; therefore, a denser monitoring network can be established, providing more information on landslide dynamics.
- The positioning quality of low-cost GNSS instruments over short baselines is comparable to high-end GNSS receivers and comes with decreased costs. Coordinate differences obtained in the static relative positioning mode between low-cost and high-end geodetic GNSS receivers are within the accuracy range of GNSS technology.
- The estimated daily coordinate differences in the static relative positioning mode in the Laze landslide did not show displacements of the measuring stations in the horizontal direction. In the vertical direction, the determined ellipsoid heights decreased over time, which could be seen more clearly in one monitoring station (ST 2). These changes were not detected in PPP due to the lower accuracy of the method itself. However, low-cost GNSS receivers can be used to achieve positioning solutions with a quality that meets landslide monitoring requirements.
- The extreme rainfall in mid-September did not trigger movements in the Laze landslide, as the coordinate differences variations obtained with LGMS were in the same range as previously observed for both horizontal and vertical components.
- Low-cost GNSS instruments are more sensitive and of lower quality compared to geodetic GNSS ones. This could lead to difficulties in data collection and consequently in the functioning of the GNSS monitoring system itself. Therefore, more reliable, rigorous, and longer tests must be conducted to evaluate their performance.
- Low-cost GNSS receivers have integrated RTK engines. The experimental test showed that these sensors can detect 20 mm spatial displacements and therefore may be suitable for developing real-time GNSS monitoring systems.
- Low-cost GNSS technology could be the solution to the increased monitoring needs caused by extreme weather events, reducing costs and thus enabling surface movements monitoring of more natural hazards in the future.

All tests were conducted to evaluate the ability of low-cost GNSS receivers for developing a low-cost GNSS monitoring system that can help to better understand and explain the surface dynamics of landslides. More tests will be performed in the future, with research focusing on automating the monitoring process and investigating data combinations from

different sensors used in landslide monitoring, for which the Laze landslide may be a suitable case study.

Author Contributions: Conceptualization, V.H.; methodology, V.H. and B.S.; software, V.H.; formal analysis, V.H.; investigation, V.H.; data curation, V.H.; writing—original draft preparation, V.H.; writing—review and editing, V.H., B.S., P.P.-P. and O.S.; visualization, V.H.; supervision, O.S., P.P.-P. and B.S. All authors have read and agreed to the published version of the manuscript.

Funding: The authors acknowledge the financial support from the Slovenian Research Agency-ARRS (research core funding no. P2-0227), Geoinformation Infrastructure and Sustainable Spatial Development of Slovenia; research core funding no. P1-0419, Dynamic Earth; and research core funding no. J2-2489 (A), SLOKIN-Geokinematic Model of Slovenian Territory.

Data Availability Statement: The data presented in this study are available on request from the corresponding author.

Acknowledgments: We are grateful to anonymous reviewers and editors for their suggestions. We acknowledge Albin Mencin for his support in the fieldwork. We are also grateful to Tomaž Beguš for the provided information and help that was necessary to perform monitoring in the Laze landslide. We are thankful to Antonino Zichichi (President of the World Federation of Scientists) and Slovenian Science Foundation for their support.

Conflicts of Interest: The authors declare no conflict of interest.

References

1. Xiao, R.; Shi, H.; He, X.; Li, Z.; Jia, D.; Yang, Z. Deformation Monitoring of Reservoir Dams Using GNSS: An Application to South-to-North Water Diversion Project, China. *IEEE Access* **2019**, *7*, 54981–54992. [CrossRef]
2. Yi, T.-H.; Li, H.-N.; Gu, M. Experimental Assessment of High-Rate GPS Receivers for Deformation Monitoring of Bridge. *Measurement* **2013**, *46*, 420–432. [CrossRef]
3. Kaloop, M.; Elbeltagi, E.; Hu, J.; Elrefai, A. Recent Advances of Structures Monitoring and Evaluation Using GPS-Time Series Monitoring Systems: A Review. *ISPRS Int. J. Geo-Inf.* **2017**, *6*, 382. [CrossRef]
4. Im, S.B.; Hurlebaus, S.; Kang, Y.J. Summary Review of GPS Technology for Structural Health Monitoring. *J. Struct. Eng.* **2013**, *139*, 1653–1664. [CrossRef]
5. Hamza, V.; Stopar, B.; Ambrožič, T.; Turk, G.; Sterle, O. Testing Multi-Frequency Low-Cost GNSS Receivers for Geodetic Monitoring Purposes. *Sensors* **2020**, *20*, 4375. [CrossRef]
6. Lin, C.; Wu, G.; Feng, X.; Li, D.; Yu, Z.; Wang, X.; Gao, Y.; Guo, J.; Wen, X.; Jian, W. Application of Multi-System Combination Precise Point Positioning in Landslide Monitoring. *Appl. Sci.* **2021**, *11*, 8378. [CrossRef]
7. Hamza, V.; Stopar, B.; Ambrožič, T.; Sterle, O. Performance Evaluation of Low-Cost Multi-Frequency GNSS Receivers and Antennas for Displacement Detection. *Appl. Sci.* **2021**, *11*, 6666. [CrossRef]
8. Ardusimple Survey Calibrated. Available online: https://www.ardusimple.com/product/calibrated-survey-gnss-multiband-antenna-ip67/ (accessed on 3 January 2023).
9. Ardusimple SimpleRTK2B. Available online: https://www.ardusimple.com/simplertk2b-receivers/ (accessed on 2 January 2023).
10. Samboko, H.T.; Schurer, S.; Savenije, H.H.G.; Makurira, H.; Banda, K.; Winsemius, H. Evaluating Low-Cost Topographic Surveys for Computations of Conveyance. *Geosci. Instrum. Method. Data Syst.* **2022**, *11*, 1–23. [CrossRef]
11. Lăpădat, A.M.; Tiberius, C.C.J.M.; Teunissen, P.J.G. Experimental Evaluation of Smartphone Accelerometer and Low-Cost Dual Frequency GNSS Sensors for Deformation Monitoring. *Sensors* **2021**, *21*, 7946. [CrossRef]
12. Romero-Andrade, R.; Trejo-Soto, M.E.; Vázquez-Ontiveros, J.R.; Hernández-Andrade, D.; Cabanillas-Zavala, J.L. Sampling Rate Impact on Precise Point Positioning with a Low-Cost GNSS Receiver. *Appl. Sci.* **2021**, *11*, 7669. [CrossRef]
13. Stępniak, K.; Paziewski, J. On the Quality of Tropospheric Estimates from Low-Cost GNSS Receiver Data Processing. *Measurement* **2022**, *198*, 111350. [CrossRef]
14. Nguyen, N.V.; Cho, W.; Hayashi, K. Performance Evaluation of a Typical Low-Cost Multi-Frequency Multi-GNSS Device for Positioning and Navigation in Agriculture—Part 1: Static Testing. *Smart Agric. Technol.* **2021**, *1*, 100004. [CrossRef]
15. Broekman, A.; Gräbe, P.J. A Low-Cost, Mobile Real-Time Kinematic Geolocation Service for Engineering and Research Applications. *HardwareX* **2021**, *10*, e00203. [CrossRef]
16. Hamza, V.; Stopar, B.; Sterle, O. Testing the Performance of Multi-Frequency Low-Cost GNSS Receivers and Antennas. *Sensors* **2021**, *21*, 2029. [CrossRef] [PubMed]
17. Janos, D.; Kuras, P. Evaluation of Low-Cost GNSS Receiver under Demanding Conditions in RTK Network Mode. *Sensors* **2021**, *21*, 5552. [CrossRef] [PubMed]
18. Wielgocka, N.; Hadas, T.; Kaczmarek, A.; Marut, G. Feasibility of Using Low-Cost Dual-Frequency GNSS Receivers for Land Surveying. *Sensors* **2021**, *21*, 1956. [CrossRef]

19. Romero-Andrade, R.; Trejo-Soto, M.E.; Vega-Ayala, A.; Hernández-Andrade, D.; Vázquez-Ontiveros, J.R.; Sharma, G. Positioning Evaluation of Single and Dual-Frequency Low-Cost GNSS Receivers Signals Using PPP and Static Relative Methods in Urban Areas. *Appl. Sci.* **2021**, *11*, 10642. [CrossRef]
20. Hamza, V.; Stopar, B.; Sterle, O.; Pavlovčič-Prešeren, P. Low-Cost Dual-Frequency GNSS Receivers and Antennas for Surveying in Urban Areas. *Sensors* **2023**, *23*, 2861. [CrossRef]
21. Krietemeyer, A.; van der Marel, H.; van de Giesen, N.; ten Veldhuis, M.-C. High Quality Zenith Tropospheric Delay Estimation Using a Low-Cost Dual-Frequency Receiver and Relative Antenna Calibration. *Remote Sens.* **2020**, *12*, 1393. [CrossRef]
22. Krietemeyer, A.; van der Marel, H.; van de Giesen, N.; ten Veldhuis, M.-C. A Field Calibration Solution to Achieve High-Grade-Level Performance for Low-Cost Dual-Frequency GNSS Receiver and Antennas. *Sensors* **2022**, *22*, 2267. [CrossRef]
23. Šegina, E.; Peternel, T.; Urbančič, T.; Realini, E.; Zupan, M.; Jež, J.; Caldera, S.; Gatti, A.; Tagliaferro, G.; Consoli, A.; et al. Monitoring Surface Displacement of a Deep-Seated Landslide by a Low-Cost and near Real-Time GNSS System. *Remote Sens.* **2020**, *12*, 3375. [CrossRef]
24. Notti, D.; Cina, A.; Manzino, A.; Colombo, A.; Bendea, I.H.; Mollo, P.; Giordan, D. Low-Cost GNSS Solution for Continuous Monitoring of Slope Instabilities Applied to Madonna Del Sasso Sanctuary (NW Italy). *Sensors* **2020**, *20*, 289. [CrossRef] [PubMed]
25. Manzini, N.; Orcesi, A.; Thom, C.; Brossault, M.-A.; Botton, S.; Ortiz, M.; Dumoulin, J. Performance Analysis of Low-Cost GNSS Stations for Structural Health Monitoring of Civil Engineering Structures. *Struct. Infrastruct. Eng.* **2020**, *18*, 595–611. [CrossRef]
26. Xue, C.; Psimoulis, P.A.; Meng, X. Feasibility Analysis of the Performance of Low-Cost GNSS Receivers in Monitoring Dynamic Motion. *Measurement* **2022**, *202*, 111819. [CrossRef]
27. Zhao, L.; Yang, Y.; Xiang, Z.; Zhang, S.; Li, X.; Wang, X.; Ma, X.; Hu, C.; Pan, J.; Zhou, Y.; et al. A Novel Low-Cost GNSS Solution for the Real-Time Deformation Monitoring of Cable Saddle Pushing: A Case Study of Guojiatuo Suspension Bridge. *Remote Sens.* **2022**, *14*, 5174. [CrossRef]
28. Barzaghi, R.; Reguzzoni, M.; De Gaetani, C.I.; Caldera, S.; Rossi, L. CULTURAL HERITAGE MONITORING BY LOW-COST GNSS RECEIVERS: A FEASIBILITY STUDY FOR SAN GAUDENZIO'S CUPOLA, NOVARA. *Int. Arch. Photogramm. Remote Sens. Spat. Inf. Sci.* **2019**, *XLII-2/W11*, 209–216. [CrossRef]
29. Poluzzi, L.; Tavasci, L.; Corsini, F.; Barbarella, M.; Gandolfi, S. Low-Cost GNSS Sensors for Monitoring Applications. *Appl. Geomat.* **2020**, *12*, 35–44. [CrossRef]
30. Tunini, L.; Zuliani, D.; Magrin, A. Applicability of Cost-Effective GNSS Sensors for Crustal Deformation Studies. *Sensors* **2022**, *22*, 350. [CrossRef]
31. Günter, J.; Heunecke, O.; Pink, S.; Schuhbäck, S. Developments towards a Low-Cost GNSS Based Sensor Network for the Monitoring of Landslides. In Proceedings of the 13th FIG International Symposium on Deformation Measurements and Analysis, Lisbon, Portugal, 12 May 2008.
32. Glabsch, J.; Heunecke, O.; Schuhbäck, S. Monitoring the Hornbergl Landslide Using a Recently Developed Low Cost GNSS Sensor Network. *J. Appl. Geod.* **2009**, *3*, 179–192. [CrossRef]
33. Komac, M.; Holley, R.; Mahapatra, P.; van der Marel, H.; Bavec, M. Coupling of GPS/GNSS and Radar Interferometric Data for a 3D Surface Displacement Monitoring of Landslides. *Landslides* **2015**, *12*, 241–257. [CrossRef]
34. Carlà, T.; Tofani, V.; Lombardi, L.; Raspini, F.; Bianchini, S.; Bertolo, D.; Thuegaz, P.; Casagli, N. Combination of GNSS, Satellite InSAR, and GBInSAR Remote Sensing Monitoring to Improve the Understanding of a Large Landslide in High Alpine Environment. *Geomorphology* **2019**, *335*, 62–75. [CrossRef]
35. Cina, A.; Piras, M. Performance of Low-Cost GNSS Receiver for Landslides Monitoring: Test and Results. *Geomat. Nat. Hazards Risk* **2015**, *6*, 497–514. [CrossRef]
36. Hohensinn, R.; Stauffer, R.; Glaner, M.F.; Herrera Pinzón, I.D.; Vuadens, E.; Rossi, Y.; Clinton, J.; Rothacher, M. Low-Cost GNSS and Real-Time PPP: Assessing the Precision of the u-Blox ZED-F9P for Kinematic Monitoring Applications. *Remote Sens.* **2022**, *14*, 5100. [CrossRef]
37. ARSO Leskovica Rain Station. Available online: https://meteo.arso.gov.si/met/sl/app/webmet/#webmet==8Sdwx2bhR2cv0WZ0V2bvEGcw9ydlJWblR3LwVnaz9SYtVmYh9iclFGbt9SaulGdugXbsx3cs9mdl5WahxXYyNGapZXZ8tHZv1WYp5mOnMHbvZXZulWYnwCchJXYtVGdlJnOn0UQQdSf (accessed on 7 November 2022).
38. Lazar, A.; Beguš, T.; Vulić, M. Integration of Measurement Techniques in Monitoring of the Laze Landslide in Slovenia. *AGS* **2020**, *17*, 33–45. [CrossRef]
39. Everett, T. RTKLIB Demo5_b33b. Available online: https://rtkexplorer.com/downloads/rtklib-code/ (accessed on 3 January 2022).
40. IGS (Institution for a Global Society). IGS Products. Available online: https://cddis.nasa.gov/archive/gnss/products/ (accessed on 2 January 2023).
41. Koch, K.-R. *Parameter Estimation and Hypothesis Testing in Linear Models*; Springer: Berlin/Heidelberg, Germany, 1999; ISBN 978-3-642-08461-4.
42. Kuang, S. *Geodetic Network Analysis and Optimal Design: Concepts and Applications*; Ann Arbor Press: Chelsea, MI, USA, 1996; ISBN 978-1-57504-044-8.

43. Caspary, W.F. *Concepts of Network and Deformation Analysis*; Monograph, 2nd. corrected impression ed.; Rüeger, J.M., Ed.; School of Surveying, University of New South Wales: Kensington, Australia, 1988; ISBN 978-0-85839-044-7.
44. Savšek, S. An Alternative Approach to Testing Displacements in a Geodetic Network. *Geod. Vestn.* **2017**, *61*, 387–411. [CrossRef]